

## Stochastic resonance in a chaotic laser

A. N. Pisarchik<sup>1,2</sup> and R. Corbalán<sup>1</sup>

<sup>1</sup>*Departament de Física, Universitat Autònoma de Barcelona, E-08193 Bellaterra, Spain*

<sup>2</sup>*Stepanov Institute of Physics, National Academy of Sciences of Belarus, Skaryna Avenue 70, 220072 Minsk, Belarus*

(Received 11 March 1998)

We report an observation of stochastic resonance in a laser with no stochastic excitation using the intrinsic chaotic dynamics. A harmonic signal in the form of a slow modulation of cavity losses is added to a loss-driven CO<sub>2</sub> laser. The signal-to-noise ratio shows a resonance in the range of the bifurcation parameter where two chaotic attractors coexist in phase space. The results of numerical simulations based on a two-level laser model are in good agreement with experiments. [S1063-651X(98)51009-4]

PACS number(s): 05.45.+b, 42.55.Lt, 42.65.Sf

### INTRODUCTION

Stochastic resonance (SR) in its classical sense is a phenomenon of an increase of the signal-to-noise ratio (SNR) with increased input noise in bistable or multistable nonlinear systems [1,2]. During the last decade this phenomenon was investigated extensively both theoretically and experimentally in a number of physical, chemical, and biological systems (for an overall review, see [3]). The basic physical mechanism underlying classical SR can be understood as follows [2]. A stochastic excitation of a lightly damped particle moving in a symmetric double-well potential leads to an exponentially decreasing Kramers time of the system jumps over the potential barrier [4]. A harmonic excitation (a signal) of the particle with a small enough amplitude that is assumed to not be able to switch the system from one well to another by itself, in the presence of noise, does do that. The coincidence of the escape rate from a well due to the stochastic excitation with the signal frequency causes a synchronization between the signal and noise that gives rise to a resonance effect in the periodic signal component and, hence, in the SNR.

Recently, SR approaches beyond classical SR have been extended to chaotic systems by keeping the noise unchanged and adding a deterministic excitation, rather than by increasing the noise [5,6]. Chaotic behavior in the system is associated with a broadband spectrum on the basis of which the output SNR is defined. It has been shown that for a certain region of the parameter space, the system switches between different chaotic repellers in relation to a periodic forcing. These intermittent hops cause the amplification of the periodic signal component in much the same manner as in classical SR. More recently, Reibold *et al.* [7] observed this so-called *noise-free* SR in ferromagnetic resonance experiments.

It is remarkable that classical SR, observed in a bidirectional ring laser ten years ago [8], provided a basis for the formulation of the theory of McNamara and Wiesenfeld [2] and its later development [3]. In this paper we report an experimental observation of the *noise-free* SR in a laser system by using the intrinsic chaotic dynamics. By exploring a domain of generalized bistability where two chaotic attractors coexist, we investigate the chaotic intermittent dynamics in a loss-driven CO<sub>2</sub> laser caused by an additive or a multi-

plicative periodic signal. Numerical simulations based on a two-level laser model are in good qualitative agreement with the experimental results and thus allow clarification of the experimental situation.

### EXPERIMENTS AND RESULTS

The experiments were carried out in a loss-driven single-mode CO<sub>2</sub> laser. The experimental setup is similar to that described in previous works [9]. The driving electric signal  $A_1 \cos(2\pi f_1 t)$  with the frequency  $f_1 = 1/T = 112$  kHz and the amplitude  $A_1$  is applied to an acousto-optic modulator providing time-dependent cavity losses. It is known [10–13] that a loss-driven CO<sub>2</sub> laser can display generalized multistability, i.e., coexistence of independent attractors in phase space at the same values of laser parameters. Varying the driving amplitude  $A_1$  from 0 to 10 V, it is possible to obtain different dynamic regimes from period 1 to chaos. These regimes can be observed in time series as well as in power spectra. We found that the first period doubling appears at  $A_1 = 1.8$  V, and at  $A_1 = 2.6$  V the dynamics of our laser becomes suddenly chaotic as one can see in the power spectrum shown in Fig. 1(a). Here,  $S$  is the power spectrum density of the laser output. The periodic structure in the power spectrum shows itself more clearly in the averaged spectrum as illustrated in Fig. 1(b). Hereafter, we analyze the power spectra taking an average of 128 Fourier transformations of separate time series. The spectral density has peaks at the fundamental excitation frequency  $f_1$ , at half driving frequency  $f_1/2$ , and a broadband portion due to the chaotic nature of the response with a maximum at  $f_1/4$ . The broadband chaotic noise indicates that the trajectory of the system resides within a chaotic attractor [9,10]. Let us suppose that some other regular or chaotic attractors can also exist for the same laser parameters. It is a very difficult problem to find the positions of these coexisting attractors experimentally but one can do it numerically [11–13] as we shall demonstrate below. Our experimental and numerical investigations show that the frequency of the maximum of broadband chaotic noise in the averaged power spectrum is a basic guideline in deciding which attractor the chaotic motion belongs to. The maximum is situated always at the frequency  $f_1/(2N)$ , where  $N$  is the number of the branch from which the chaotic attractor develops. For example, if the maximum of broad-

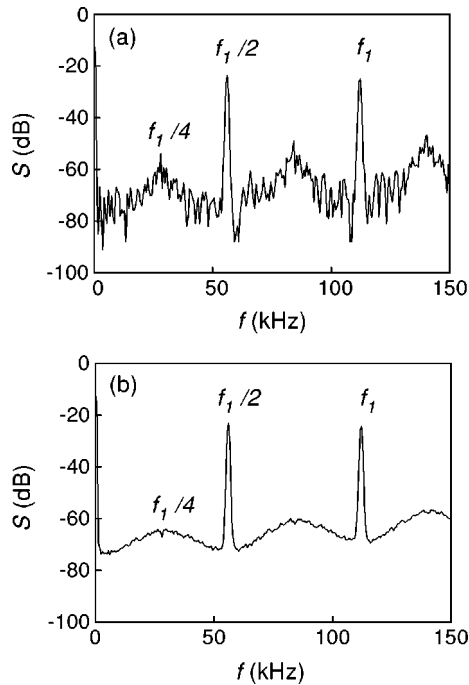


FIG. 1. Experimental power spectra of a CO<sub>2</sub> laser in the chaotic regime associated with a period-2 branch of orbits. (a) Spectrum from a single time series. (b) Spectrum averaged over 128 realizations.

band noise is situated at the frequency  $f_1/2$ , the chaotic regime belongs to the attractor developed from a period-1 branch of orbits. On the other hand, if the frequency of the maximum is equal to  $f_1/6$ , chaos is associated with a period-3 branch. In the case illustrated in Fig. 1(b) the laser operates in the chaotic regime of a period-2 branch attractor.

Since different stable attractors can coexist, and given the existence in the spectrum of a broadband portion similar to that in the case of classical SR, it is possible to organize intermittent jumps between the attractors by applying an additional small periodic modulation of a laser parameter. The intrinsic chaotic dynamics (the broadband noise) performs a synchronization phenomenon that acts in much the same manner as for stochastic noise in classical SR [5–7]. To obtain the resonance effect we add a slow modulation of the cavity losses. Accordingly, the combined voltage applied to the modulator is now

$$G(t) = A_1 \cos(2\pi f_1 t) + A_2 \cos(2\pi f_2 t), \quad (1)$$

where  $A_1 \cos(2\pi f_1 t)$  is the driving modulation with amplitude  $A_1$  and frequency  $f_1 = 112$  kHz, and  $A_2 \cos(2\pi f_2 t)$  is the *additive* external deterministic force (signal) with amplitude  $A_2$  and frequency  $f_2 = 10$  kHz ( $f_2 \ll f_1$ ). The power spectra of the laser output in the presence of the modulation [Eq. (1)] are displayed in Fig. 2 for three values of the driving amplitude  $A_1$  in the range of chaos. The additional loss modulation is chosen to be large enough to observe a periodic component at  $f_2$  in the laser response. In fact, the amplitude of the additional modulation  $A_2 = 10$  V is not small when compared with the driving  $A_1$ , but the effects of the frequencies  $f_1$  and  $f_2$  on the output are different. The imbalance between input and output signals appears because the

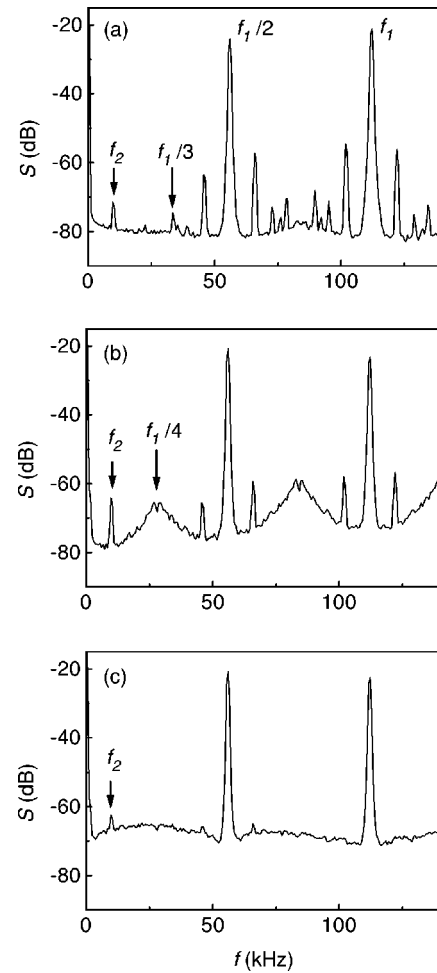


FIG. 2. Experimental averaged power spectra of a CO<sub>2</sub> laser with no stochastic excitation and with slow additive modulation of cavity losses at  $f_2$  for different driving amplitudes (a)  $A_1 = 2.8$  V, (b) 3.2 V, and (c) 3.8 V.

modulator has a strong acoustic resonance at 112 kHz while at 10 kHz the modulator is weakly efficient. As a result, at  $A_1 = 1$  V and  $A_2 = 10$  V the laser response at  $f_2$  is 100 times smaller than that at  $f_1$ .

One can see from Fig. 2 that the periodic component at  $f_2 = 10$  kHz, together with a set of difference frequencies, arise in the spectra. The  $f_2$  spectral component  $S(f_2) = S_g(f_2) + S_n(f_2)$  is composed of two contributions: a chaotic broadband portion  $S_n(f_2)$  and a signal  $S_g(f_2)$ . Comparing these spectra for different  $A_1$ , one can see that the signal amplitude  $S_g(f_2)$  is enhanced at  $A_1 = 3.2$  V [Fig. 2(b)] with respect to their respective counterparts in Figs. 2(a) and 2(c), for which  $A_1 = 2.6$  V and 3.8 V. This is because of the resonance due to the intrinsic chaotic dynamics; the level of chaotic broadband portion increases with increasing  $A_1$ . The presence of the  $f_1/3$  component and  $f_1/4$  component in the spectra in Figs. 2(a) and 2(b), respectively, is good circumstantial evidence that at least two chaotic attractors coexist for the range of the driving amplitudes exploited in Fig. 2.

Figure 3(a) shows the dependence of the SNR at  $f_2$  on  $A_1$  for the additive signal given by Eq. (1). In this paper we define the SNR ( $\mathcal{R}$ ) as the relationship

$$\mathcal{R} = 10 \log \frac{S_g(f_2) + S_n(f_2)}{S_n(f_2)}. \quad (2)$$

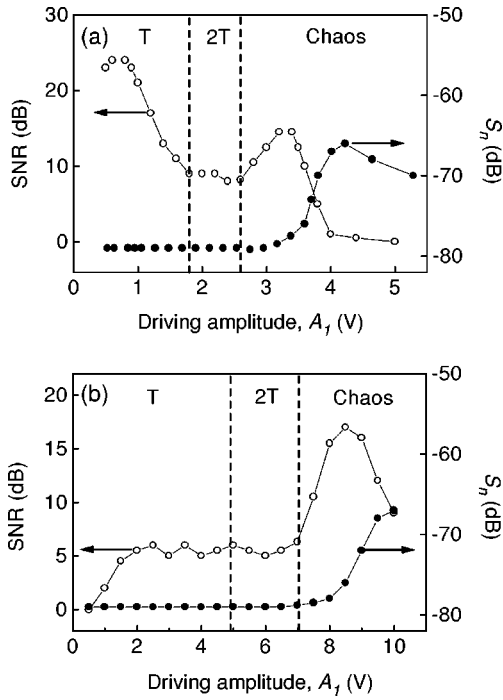


FIG. 3. Experimental signal-to-noise ratio (open circles) and power density of the broadband portion (closed circles) vs the driving voltage  $A_1$ . (a) Additive signal corresponding to Eq. (1). (b) Multiplicative signal corresponding to Eq. (3);  $f_1 = 112$  kHz and  $f_2 = 10$  kHz. The vertical dashed lines show the positions of the bifurcation boundaries in the absence of additional modulation.

In Fig. 3(a) we also show how the level of the broadband portion  $S_n(f_2)$  depends on  $A_1$ . The vertical dashed lines indicate the locations of the bifurcation boundaries without the additional modulation, i.e., when  $A_2 = 0$ . One can see that the SNR has a resonance at  $A_1 \approx 3.2$  V where the motion is chaotic and  $S_n$  increases. At  $A_1 > 2.6$  V the laser operates in a “chaos-chaos” intermittency regime where two chaotic attractors,  $2T$  and  $3T$ , coexist in phase space. This can be seen from the power spectra shown in Fig. 2. The additional slow modulation provides synchronized switches between these two coexisting attractors.

A similar resonance effect is also observed when we modulate the maximal amplitude of the driving force, i.e., when we apply a *multiplicative* signal so that the total voltage is

$$G(t) = A_1 [1 + m \cos(2\pi f_2 t)] \cos(2\pi f_1 t), \quad (3)$$

where  $m$  is the modulation depth. Such a signal is much easier to implement experimentally because it can be generated from a single generator with additional amplitude modulation. Figure 3(b) displays the SNR and broadband portion  $S_n(f_2)$  versus  $A_1$  for the signal [Eq. (3)] at  $m = 0.3$ . Thus, in both cases the SNR has the resonance at some level of the broadband chaotic noise that provides the synchronization phenomenon noted for classical SR.

## NUMERICAL SIMULATIONS

We use the following two-level rate-equation laser model [10,14]:

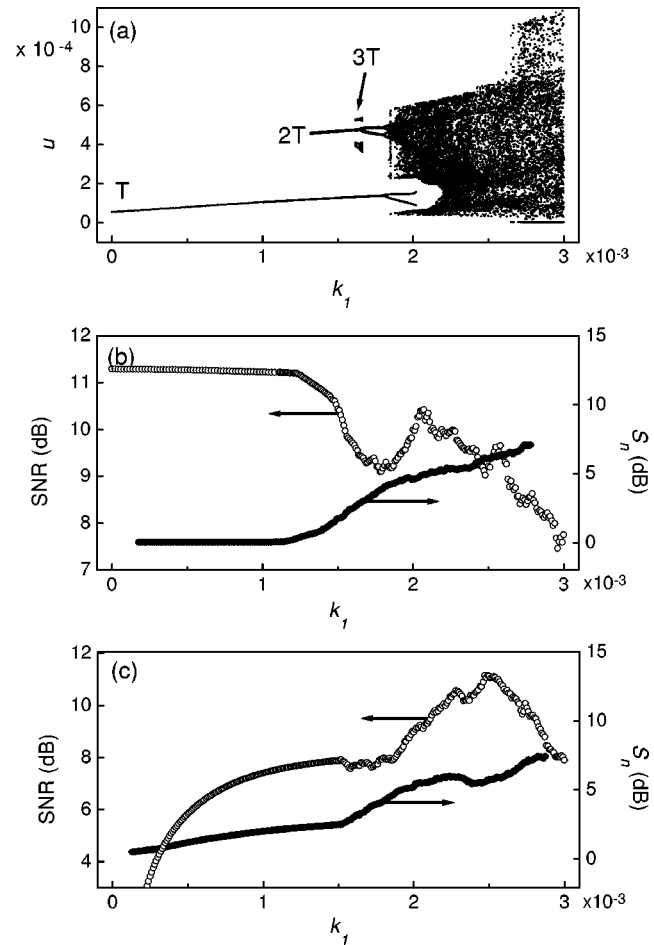


FIG. 4. (a) Numerical bifurcation diagram of the  $u$  function of the driving amplitude. Stable branches of the period-1, -2, and -3 orbits are marked by the letters  $T$ ,  $2T$ , and  $3T$ . (b) and (c) SNR (open circles) and power spectrum density of the broadband portion (closed circles) vs the driving amplitude for (b) additive signal [Eq. (5)], and (c) multiplicative signal [Eq. (6)].

$$\frac{du}{dt} = \tau^{-1}(y - k_0 - k)u, \quad \frac{dy}{dt} = (y_0 - y)\gamma - uy. \quad (4)$$

Here  $u$  is proportional to the radiation density,  $y$  and  $y_0$  are the gain and the unsaturated gain in the active medium, respectively,  $\tau$  is half of the round-trip time of light in the resonator,  $\gamma$  is the gain decay rate, and  $k_0$  is the constant part of the losses. Analogous to what is done in the experiments, the variable cavity losses are changed either by adding a slow signal  $k_2 \cos(2\pi f_2 t)$  to a driving force  $k_1 \cos(2\pi f_1 t)$ , so that

$$k = k_1 \cos(2\pi f_1 t) + k_2 \cos(2\pi f_2 t), \quad (5)$$

where  $k_1$  and  $k_2$  are the driving and signal amplitudes respectively, or by an additional modulation of the driving amplitude

$$k = k_1 [1 + m \cos(2\pi f_2 t)] \cos(2\pi f_1 t). \quad (6)$$

Equations (5) and (6) thus simulate the experimental situations with the additive and multiplicative signals as defined by Eqs. (1) and (3). To better model the experimental situa-

tion we take the numerical parameters to be close to the experimental ones. To this aim we fix the parameters throughout our calculations:  $\tau=3.5\times 10^{-9}$  s,  $\gamma=10^5$  s $^{-1}$ ,  $y_0=0.1805$ ,  $k_0=0.173$ ,  $f_1=112$ ,  $f_2=10$  kHz, while the parameters  $k_1$ ,  $k_2$ , and  $m$  are varied in the numerical simulations.

Figure 4(a) shows the bifurcation diagram obtained with different initial conditions without additional signal ( $k_2=0$  or  $m=0$ ). One can see that the system of Eq. (4) has several stable solutions or coexisting attractors at  $k_1>1.3\times 10^{-3}$ . For instance, a period-2 branch of orbits ( $2T$ ) appears at  $k_1\approx 1.3\times 10^{-3}$ , then a period-3 branch ( $3T$ ) arises at  $k_1\approx 1.6\times 10^{-3}$ , and finally at  $k_1\approx 1.8\times 10^{-3}$  these attractors become chaotic and overlap. The application of the additional loss modulation with  $f_2=10$  kHz and  $k_2=10^{-4}$  or  $m=0.3$  provides a synchronization effect that shows up as the resonance in the SNR as shown in Figs. 4(b) and 4(c) for the signals corresponding to Eqs. (5) and (6), respectively. All SNR calculations in this paper are based on Eq. (2). In Figs. 4(b) and 4(c) we also plot the dependences of the broadband portion  $S_n(f_2)$  on  $k_1$ . Each point in Figs. 4(b) and 4(c) is an average over 20 neighborhood points recorded at different  $k_1$  with a step of  $\Delta k_1=10^{-5}$ . In Fig. 4(b) the broadband portion begins to increase at  $k_1\approx 1.3\times 10^{-3}$  just when the  $2T$  branch of period-doubling orbits appears in the bifurcation diagram. Increasing  $S_n$  leads first to the diminution of the SNR and then to the resonance in the SNR. This resonance arises in the domain where two chaotic attractors associated with the  $2T$  and  $3T$  branches coexist, and the signal at  $f_2$  provides

synchronized switches between these attractors. Comparing the numerical plots shown in Figs. 4(b) and 4(c) with the experimental dependences displayed in Figs. 3(a) and 3(b) one can see that the agreement is remarkably good. This demonstrates that the SR approach can be used as an effective experimental instrument to detect coexisting attractors among other experimental methods such as targeting technique [15] and dynamical tracking periodic orbits [16].

## CONCLUSION

To conclude, we have reported on experimentally and numerically obtained noise-free stochastic resonance in a chaotic CO<sub>2</sub> laser due to the intrinsic chaotic dynamics. A broadband portion of the output power spectrum acts very similar to a deterministic noise in classical SR; the laser switches in phase space between coexisting attractors. The enhancement of the SNR is achieved by adding either an additive or a multiplicative harmonic signal while leaving the noise unchanged. We expect that noise-free stochastic resonance will also be realized in other lasers that admit the coexistence of different attractors. The observed phenomenon can be of interest for communications with lasers.

## ACKNOWLEDGMENTS

This work has been supported by DGICYT (Spain) (Project No. PB95-0778). A.N.P. acknowledges support from the Ministerio de Educación y Cultura, Spain (Project No. SAB94-0538).

- 
- [1] R. Benzi, A. Sutera, and A. Vulpiani, *J. Phys. A* **14**, L453 (1981).
  - [2] B. McNamara and K. Wiesenfeld, *Phys. Rev. A* **39**, 4854 (1989).
  - [3] K. Weisenfeld and F. Moss, *Nature (London)* **373**, 33 (1994); M. I. Dykman *et al.*, *Nuovo Cimento D* **17**, 661 (1995); L. Gammaitoni *et al.*, *Rev. Mod. Phys.* (to be published).
  - [4] H. A. Kramers, *Physica (Utrecht)* **7**, 284 (1940).
  - [5] V. S. Anishchenko, A. B. Neiman, and M. A. Safanova, *J. Stat. Phys.* **70**, 183 (1993).
  - [6] M. Franaszek and E. Simiu, *Phys. Rev. E* **54**, 1298 (1996).
  - [7] E. Reibold, W. Just, J. Becker, and H. Benner, *Phys. Rev. Lett.* **78**, 3101 (1997).
  - [8] B. McNamara, K. Wiesenfeld, and R. Roy, *Phys. Rev. Lett.* **60**, 2626 (1988).
  - [9] A. N. Pisarchik, V. N. Chizhevsky, R. Corbalán, and R. Vilaseca, *Phys. Rev. E* **55**, 2455 (1997); A. N. Pisarchik, B. F. Kuntsevich, and R. Corbalán, *ibid.* **57**, 4046 (1998).
  - [10] F. T. Arecchi, R. Meucci, G. Puccioni, and J. Tredicce, *Phys. Rev. Lett.* **49**, 1217 (1982); J. R. Tredicce, F. T. Arecchi, G. P. Puccioni, A. Poggi, and W. Gadomski, *Phys. Rev. A* **34**, 2073 (1986).
  - [11] H. G. Solari, E. Eschenazi, R. Gilmore, and J. R. Tredicce, *Opt. Commun.* **64**, 49 (1987).
  - [12] I. B. Schwartz, *Phys. Rev. Lett.* **60**, 1359 (1988).
  - [13] P. Glorieux, C. Lepers, R. Corbalán, J. Cortit, and A. N. Pisarchik, *Opt. Commun.* **118**, 309 (1995).
  - [14] V. N. Chizhevsky, R. Corbalán, and A. N. Pisarchik, *Phys. Rev. E* **56**, 1580 (1997).
  - [15] V. N. Chizhevsky and P. Glorieux, *Phys. Rev. E* **51**, R2701 (1995).
  - [16] A. N. Pisarchik, *Phys. Lett. A* **242**, 152 (1998).